We are IntechOpen,
the world's leading publisher of
Open Access books
Built by scientists, for scientists

6,900
Open access books available

185,000
International authors and editors

200M
Downloads

Our authors are among the

154
Countries delivered to

TOP 1%
most cited scientists

12.2%
Contributors from top 500 universities

CLARIVATE ANALYTICS
BOOK CITATION INDEX
INDEXED

WEB OF SCIENCE™

Selection of our books indexed in the Book Citation Index
in Web of Science™ Core Collection (BKCI)

Interested in publishing with us?
Contact book.department@intechopen.com

Numbers displayed above are based on latest data collected.
For more information visit www.intechopen.com

Wettability on Different Surfaces

Yeeli Kelvii Kwok

Abstract

Wettability has been explored for 100 years since it is described by Young's equation in 1805. It is all known that hydrophilicity means contact angle (θ), $\theta < 90°$; hydrophobicity means contact angle (θ), $\theta > 90°$. The utilization of both hydrophilic surfaces and hydrophobic surfaces has also been achieved in both academic and practical perspectives. In order to understand the wettability of a droplet distributed on the textured surfaces, the relevant models are reviewed along with understanding the formation of contact angle and how it is affected by the roughness of the textured surface aiming to obtain the required surface without considering whether the original material is hydrophilic or hydrophobic.

Keywords: wettability, droplet, hydrophilic, hydrophobic, surface tension, contact angle, textured surface, Wenzel model, Cassie-Baxter model

1. Introduction

It is well known that when a small droplet of liquid is deposited on the solid surface, it forms a shape with a contact angle to the solid. This phenomenon is firstly described by Young in 1805, and he proposed that surface energy is the interaction between the forces of adhesion and the forces of cohesion which determine whether the wetting occurs or not (i.e., the spreading of a liquid over a surface) [1]. If it does not occur the complete wetting, the liquid in a bead shape will be formed. In the same time, as a function of the surface energies, a contact angle is defined in the system.

When the liquid wets the solid, three different interfacial boundary surfaces, viz., solid-air (sv), solid-liquid (sl), and liquid-air (lv), are involved. The contact angle, which is included between the interfaces of sl and lv, has to reach a certain value to satisfy the equilibrium state of the three interfacial tensions. It is all known that there are two requirements for the equilibrium.

2. Static equilibrium

The first requirement for keeping a balance of the three interfacial tensions in horizontal direction is described by Young's Eq. (1):

$$\gamma_{lv} \cos\theta = \gamma_{sv} - \gamma_{sl} \qquad (1)$$

where γ denotes the interfacial tension in the denomination of the force per unit length, or of the energy per unit area, which are equivalent in measuring the surface energy density, and θ is the contact angle at a location where the tangent along an lv
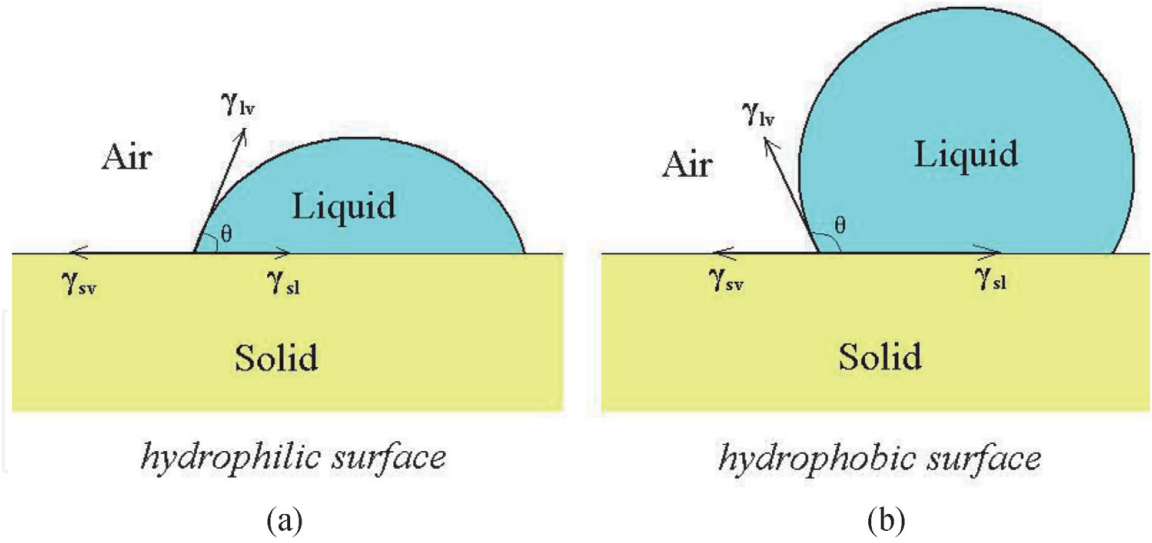
Figure 1.
Contact angle on various surfaces.

interface intersects the solid surface as shown in **Figure 1**. For the surface of solid with high surface energy, $\gamma_{sv} > \gamma_{sl}$, γ_{lv} directs to the side of γ_{sl} and forms a contact angle smaller than 90°. This kind of surface is known to be hydrophilic as shown in **Figure 1a**. For a solid with low surface energy, $\gamma_{sv} < \gamma_{sl}$, γ_{lv} directs to the side of γ_{sv} and forms a contact angle larger than 90° which is known to be hydrophobic as shown in **Figure 1b**.

3. Dynamic equilibrium

Another requirement is the dynamic equilibrium determined by the interface energy which can be calculated from $\gamma \times s$, where s is the area of interface. It should be noted that for a droplet of liquid with certain volume resting on a solid surface, it has the smallest lv interface when the contact angle is 90° (i.e., the droplet is a hemisphere as shown by the blue quarter circle in **Figure 2**); and whether its sl interface spreads (i.e., θ decreases) when $\theta < 90°$ or contract to be more like a sphere (i.e., θ increases) when $\theta > 90°$, the lv interface area increases. Firstly, considering a droplet on a hydrophilic solid surface as shown in **Figure 2a**, the shape of the droplet has not reached equilibrium. With the spreading of the liquid, the area of both the sl interface and the lv interface will increase simultaneously. Because $\gamma_{sv} > \gamma_{sl}$ on hydrophilic surface, the increment of the sl interface area means the conversion from the sv interface to the sl interface. The process involves a release in energy from the sv interface to the sl interface; as a result, the increment of the lv interface area implies a consumption of energy. When the energy changes caused by these two contrary factors are equal, the shape of the droplet will settle and the contact angle will achieve the final value of θ. This energy equilibrium can be described by the following equation:

$$(\gamma_{sv} - \gamma_{sl})ds_{sl} = \gamma_{lv}ds_{lv} \qquad (2)$$

where ds_{sl} and ds_{lv} mean a slight variation in the area of sl interface and lv interface, respectively. By combining with Eq. (1), the contact angle can be expressed by:

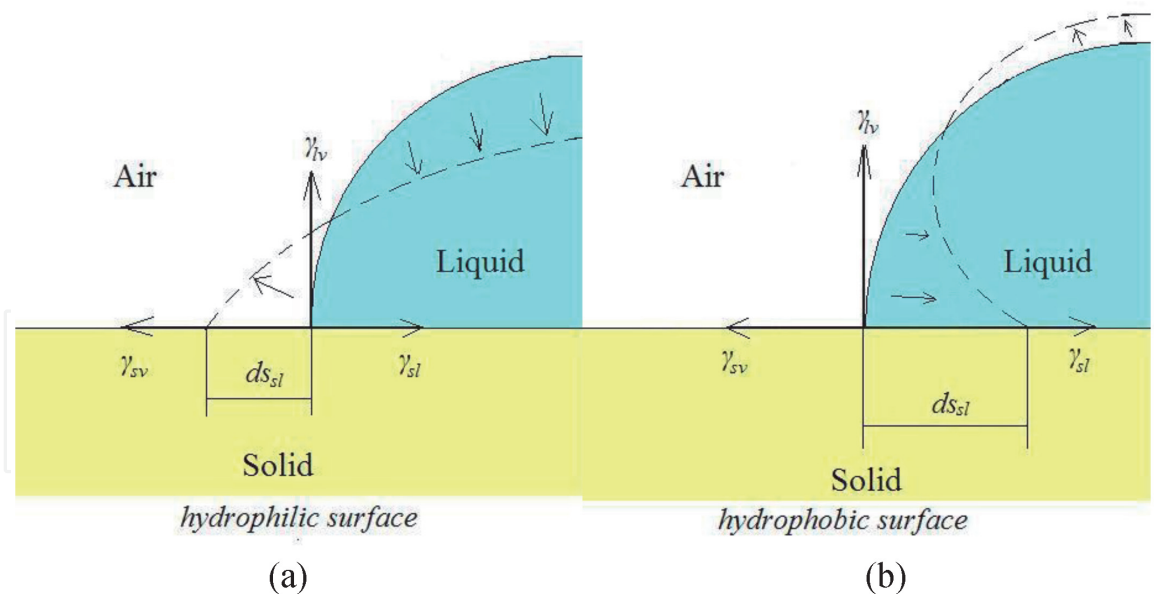$$\cos\theta = \frac{ds_{lv}}{ds_{sl}} \qquad (3)$$

Figure 2.
Drop of liquid on solid surfaces when the equilibrium has not been reached.

It should be noticed that ds_{lv}/ds_{sl} is the area changing rate of the lv interface with the sl interface increasing; it is only determined by the shape of the droplet. Eq. 3 shows the relationship between the contact angle and the profile of the droplet and is independent of materials and surface tension.

For the system applied on a hydrophobic surface as shown in **Figure 2b**, with the effect of the contracting of liquid, the area of the sl interface decreases with increasing lv interface. Because $\gamma_{sv} < \gamma_{sl}$ on hydrophobic surface, the decrement of the sl area involves a release of energy to the increasing lv interface area. When the dynamic equilibrium of energy is reached, Eqs. (2) and (3) can also be applied on this kind of surface.

$$-(\gamma_{sv} - \gamma_{sl})(-ds_{sl}) = \gamma_{lv}ds_{lv} \qquad (4)$$

$$\cos\theta = \frac{ds_{lv}}{ds_{sl}}$$

It should be noted that (γ_{sv}-γ_{sl}) and ds_{sl} are negative on hydrophobic surface.

4. Effect of surface roughness on contact angle

It should be noticed that there distinctively exists a difference between the geometric surface and the actual surface and their interface is not ideal as a pro-posed model in the textbooks. Actually, the surface of any real solid is not a perfect plane. Due to the surface roughness, the real area of the actual surface is larger than the so-called ideal (geometric) surface. Consequently, the surface roughness affects the contact angle and the contact angle distinctively varies with the surface rough-ness. As a result, in order to keep the equilibrium, the profile of a droplet will vary with the effect of the surface roughness. For studying θ' (new contact angle) distributed on the real rough surface and the effect of its roughness on the relevant wettability, Wenzel and Cassie-Baxter proposed two different models to explain as a key effective factor how solid surfaces with the real geometry features affect the wettability [2–8].

Wenzel model.

According to the model described by Wenzel in 1936 [9], the solid surface completely contacts with liquid under the droplet as shown in **Figure 3**. The *sl* interface area is enlarged to be s'_{sl} which is equal to the "actual surface" by the roughness. There is a ratio of the sl interface area to the geometric surface area, *r*, which is larger than 1.

$$s'_{sl} = rs_{sl} \tag{5}$$

With a variation of the geometric *sl* interface area, the amount of energy released from it or accumulated in it is increased:

$$(\gamma_{sv} - \gamma_{sl})ds'_{sl} = r(\gamma_{sv} - \gamma_{sl})ds_{sl} \tag{6}$$

In addition, the lv interface is not affected by the surface roughness. So the equilibrium with the new contact angle of θ' can be expressed by:

$$\cos \theta' = \frac{r(\gamma_{sv} - \gamma_{sl})}{\gamma_{lv}} \tag{7}$$

Compared with Eq. (1), θ' can be depicted as:

$$\cos \theta' = r \cos \theta \tag{8}$$

Taken θ_w and θ_0 to represent θ' and θ, respectively, it is obtained:

$$\cos \theta_w = r \cos \theta_0 \tag{9}$$

where θ_w is the contact angle on the rough surface with Wenzel model and θ_0 is the original contact angle according to the ideal smooth surface. Eq. 9 is the Wenzel equation. It shows that when Wenzel model is applied, $r > 1$, the morphology of the surface always magnifies the underlying wetting properties. θ_w is larger than θ_0 for the hydrophobic material ($\theta_0 > 90°$); and it is smaller than θ for the hydrophilic material ($\theta_0 < 90°$) [10–12].
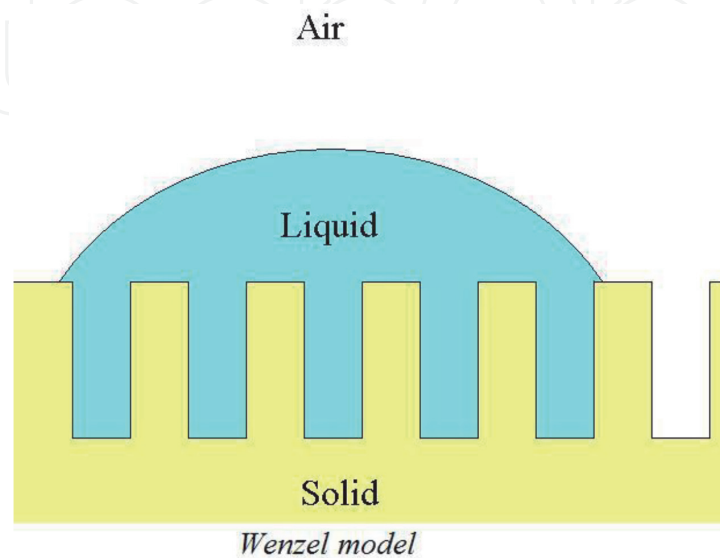

Figure 3.
Schematic of a droplet on the rough surface described by Wenzel.

5. Cassie-Baxter model

In 1944, Cassie applied and explored Wenzel equation on porous materials [13]. According to Cassie-Baxter model, air can be trapped below the drop as shown in **Figure 4**. The area of the *sl* interface is reduced by the surface roughness while a part of that transits to the lv interface in indentations. The ratio of the actual *sl* interface area to the geometric surface area is represented by f, which is smaller than 1 in Cassie-Baxter model.

$$ds'_{sl} = fds_{sl} \tag{10}$$

$$ds'_{lv} = ds_{lv} + (1-f)ds_{sl} \tag{11}$$

With a variation of the profile of the droplet, the amount of energy transited among the interfaces is changed:

$$(\gamma_{sv} - \gamma_{sl})ds'_{sl} = f(\gamma_{sv} - \gamma_{sl})ds_{sl} \tag{12}$$

$$\gamma_{lv}ds'_{lv} = \gamma_{lv}ds_{lv} + (1-f)\gamma_{lv}ds_{sl} \tag{13}$$

The equilibrium with the new contact angle of θ' can be expressed by:

$$\cos\theta' = \frac{f(\gamma_{sv} - \gamma_{sl})}{\gamma_{lv}} - (1-f) \tag{14}$$

Compared with Eq. (1), θ' can be calculated as:

$$\cos\theta' = f(\cos\theta + 1) - 1 \tag{15}$$

Taken θ_c and θ_0 to represent θ' and θ, respectively, it is obtained:

$$\cos\theta_c = f(\cos\theta_0 + 1) - 1 \tag{16}$$

where θ_c is the contact angle on rough surface with Cassie-Baxter model. Eq. (16) is Cassie-Baxter equation. According to Cassie-Baxter model, only the

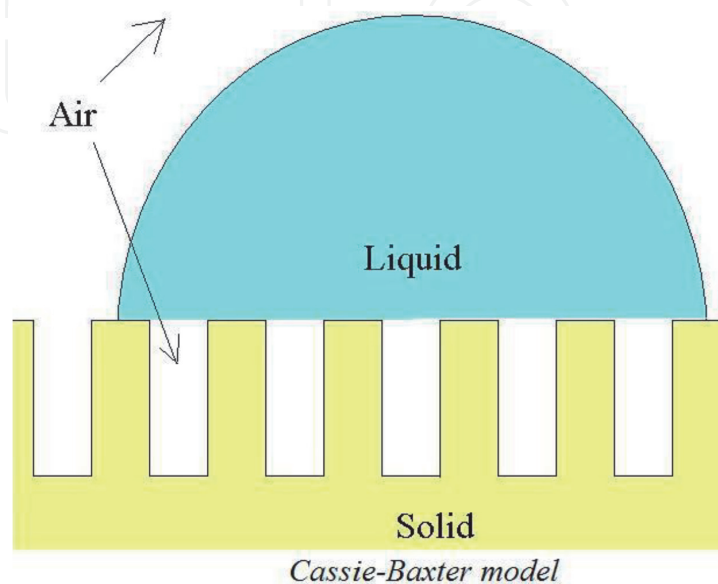Cassie-Baxter model

Figure 4.
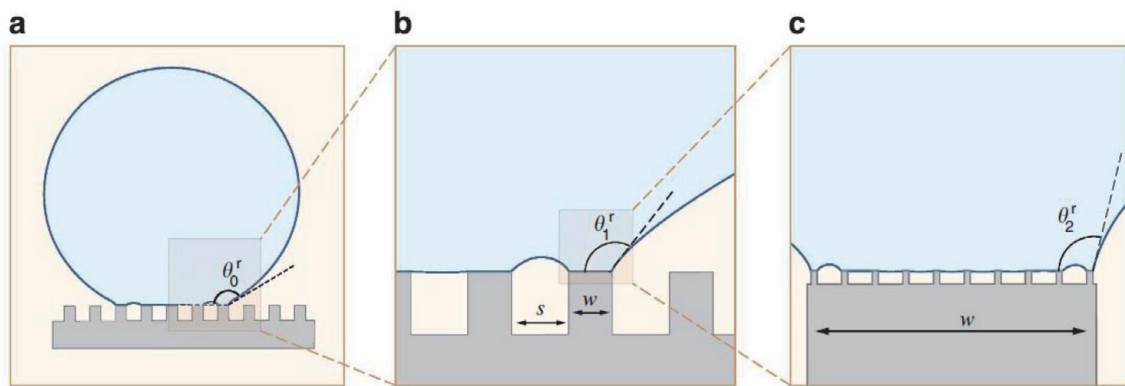*Schematic of a droplet on the rough surface described by Cassie-Baxter.*

Figure 5.
Schematic of self-similar contact line pinning. (a) A liquid droplet that rests in a Cassie-Baxter state on a hierarchical surface exhibits an apparent receding angle θ_0^r. (b) The apparent contact line of the drop is divided into many smaller first-level contact lines, each at the top of a first-level roughness feature with width w and spacing s. each of these first-level contact lines sits at the base of a first-level capillary bridge, which has a local receding contact angle θ_1^r. (c) The apparent contact line of each second-level capillary bridge is further divided into smaller second-level contact lines, each atop a second-level roughness feature. Each second-level contact line sits at the base of a second-level capillary bridge, which has a local receding contact angle θ_2^r.

characteristics of hydrophobicity can be enhanced. θ_c is always larger than θ on the rough surface [14–17].

In fact, numerous investigations have been devoted to the wettability on different surfaces, particularly for the surfaces inspired by Nature Mother [18–26]. Paxson et al. [27] fabricated a surface with the hierarchical textures initiated by lotus leaves and revealed the relevant mechanism of the variation or evolution of the adhesion force per unit length of the projected contact line distributed on natural textured surfaces. Results show that the adhesion force varies with the pinned fraction of each level of hierarchy.

Figure 5 shows a droplet sitting on a textured surface in a Cassie-Baxter state. It depicts the real contact line of the droplet, which is changed into many smaller lines. Meanwhile, the contact angle also changes from θ_0^r (the zeroth level) to θ_1^r (the first level of hierarchy) as shown in **Figure 5b**. If the contact line is divided into much smaller lines, viz., the second level of hierarchy, the related contact angle θ_2^r is distinctively different from θ_1^r of the first level of hierarchy as shown in **Figure 5c**. These phenomena will be kept on until a homogeneous wetting interface achieved when reaching a level *n*. Consequently, the contact angle either increases or decreases by adding multiple length scales of roughness at all smaller levels depending on the pinned fraction of each level of hierarchy, which is critical for designing surfaces with various adhesion [28–33].

6. Conclusion

The droplet on a solid surface will exhibit a certain value of contact angle to achieve the equilibrium of the interfacial tensions. In addition, surface roughness will influence the contact angle, based on Wenzel's and Cassie-Baxter's theories, with the assumption of overhangs. It reveals that the contact angle can be controlled by the intentionally fabricated textured surfaces, and the surface with the fabricated textures can be changed from hydrophilic to hydrophobic, and vice versa, without considering whether the original material is hydrophilic or hydrophobic.

Author details

Yeeli Kelvii Kwok
Department of Mechanical and Biomedical Engineering, City University of Hong Kong, Kowloon, Hong Kong

*Address all correspondence to: yeelikwok@yahoo.com

IntechOpen

References

[1] Young T. An essay on the cohesion of fluids. Philosophical Transactions: Royal Society London. 1805;**95**:65-87

[2] Bormashenko E, Bormashenko Y, Stein T, Whyman G, Bormashenko E. Why do pigeon feathers repel water? Hydrophobicity of pennae, Cassie-Baxter wetting hypothesis and Cassie-Wenzel capillarity-induced wetting transition. Journal of Colloid and Interface Science. 2007;**311**(11):212-216

[3] Whyman G, Bormashenko E, Stein T. The rigorous derivation of Young, Cassie-Baxter and Wenzel equations and the analysis of the contact angle hysteresis phenomenon. Chemical Physics Letters. 2008;**450**(4–64): 355-359

[4] Elif Cansoy C, Yildirim Erbil H, Akar O, Akin T. Effect of pattern size and geometry on the use of Cassie-Baxter equation for superhydrophobic surfaces. Colloids and Surfaces A: Physicochemical and Engineering Aspects. 2011;**386**(1–35):116-124

[5] Parry V, Berthomé G, Joud JC. Wetting properties of gas diffusion layers: Application of the Cassie-Baxter and Wenzel equations. Applied Surface Science. 2012;**258**(1515):5619-5627

[6] Lee J, Hwang SH, Yoon SS, Khang DY. Evaporation characteristics of water droplets in Cassie, Wenzel, and mixed states on superhydrophobic pillared Si surface. Colloids and Surfaces A: Physicochemical and Engineering Aspects. 2019;**5625**:304-309

[7] Montes Ruiz-Cabello FJ, Cabrerizo-Vílchez MA, Rodríguez-Valverde MA. Evaluation of the solid-liquid contact area fraction of drops deposited on rough surfaces beyond the Wenzel regime. Colloids and Surfaces A: Physicochemical and Engineering Aspects. 2019;**5685**:455-460

[8] Bormashenko E. Progress in understanding wetting transitions on rough surfaces. Advances in Colloid and Interface Science. 2015;**222**:92-103

[9] Wenzel RN. Resistance of solid surfaces to wetting by water. Journal of Industrial and Engineering Chemistry. 1936;**28**:988-994

[10] Bormashenko E. General equation describing wetting of rough surfaces. Journal of Colloid and Interface Science. 2011;**360**(11):317-319

[11] Khilifi D, Foudhil W, Harmand S, Jabrallah SB. Evaporation of a sessile oil drop in the Wenzel-like regime. International Journal of Thermal Sciences. 2020;**151**:106236

[12] Ceyhan U, Tiktaş A, Özdoğan M. Pinning and depinning of Wenzel-state droplets around inclined steps. Colloid and Interface Science Communications. 2020;**35**:100238

[13] Cassie ABD. Wettability of porous surfaces. Transactions of the Faraday Society. 1944;**40**:546-551

[14] Milne AJB, Amirfazli A. The Cassie equation: How it is meant to be used. Advances in Colloid and Interface Science. 2012;**170**(1–215):48-55

[15] Cengiz U, Elif CC. Applicability of Cassie-Baxter equation for superhydrophobic fluoropolymer-silica composite films. Applied Surface Science. 2015;**33530**:99-106

[16] Aziz H, Amrei MM, Dotivala A, Tang C, Vahedi TH. Modeling Cassie droplets on superhydrophobic coatings with orthogonal fibrous structures. Colloids and Surfaces A: Physicochemical and Engineering Aspects. 2017;**5121**:61-70

[17] Rivera RM, Koltsov A, Lazcano BA, Douce JF. Wettability in water/iron ore

powder systems: To the universality of the Cassie model. International Journal of Mineral Processing. 2017;**16210**:36-47

[18] Malvadkar NA, Hancock MJ, Sekeroglu K, Dressick WJ, Demirel MC. An engineered anisotropic nanofilm with unidirectional wetting properties. Nature Materials. 2010;**9**:1023-1028

[19] Raj R, Adera S, Enright R, Wang EN. High-resolution liquid patterns via three-dimensional droplet shape control. Nature Communications. 2014;**5**:4975

[20] Kreder MJ, Alvarenga J, Kim P, Aizenberg J. Design of anti-icing surfaces: Smooth, textured or slippery? Nature Reviews Materials. 2016;**1**:15003

[21] Schneider L, Laustsen M, Mandsberg N, Taboryski R. The influence of structure heights and opening angles of micro- and nanocones on the macroscopic surface wetting properties. Scientific Reports. 2016;**6**: 21400

[22] Ujjain SK, Roy PK, Kumar S, Singha S, Khare K. Uniting superhydrophobic, superoleophobic and lubricant infused slippery behavior on copper oxide nano-structured substrates. Scientific Reports. 2016;**6**: 35524

[23] Lo YH, Yang CY, Chang HK, Hung WC, Chen PY. Bioinspired diatomite membrane with selective superwettability for oil/water separation. Scientific Reports. 2017;7:1426

[24] Ivanchenko P, Delgado-López JM, Iafisco M, Gómez-Morales J, Tampieri A, Martra G, et al. On the surface effects of citrates on nano-apatites: Evidence of a decreased hydrophilicity. Scientific Reports. 2017; 7:8901

[25] Lee Y, Matsushima N, Yada S, Nita S, Kodama T, Amberg G, et al. Revealing how topography of surface microstructures alters capillary spreading. Scientific Reports. 2019;**9**:7787

[26] Wong TS, Kang SH, Tang SKY, Smythe EJ, Hatton BD, Grinthal A, et al. Bioinspired self-repairing slippery surfaces with pressure-stable omniphobicity. Nature. 2011;**477**: 443-447

[27] Paxson AT, Varanasi KK. Self-similarity of contact line depinning from textured surfaces. Nature Communications. 2013;**4**:1492

[28] Kubiak KJ, Wilson MCT, Mathia TG, Carval P. Wettability versus roughness of engineering surfaces. Wear. 2011;**271**(3–43):523-528

[29] Sarkar A, Kietzig A-M. General equation of wettability: A tool to calculate the contact angle for a rough surface. Chemical Physics Letters. 2013; **57414**:106-111

[30] Bormashenko E. Apparent contact angles for reactive wetting of smooth, rough, and heterogeneous surfaces calculated from the variational principles. Journal of Colloid and Interface Science. 2019;**5371**:597-603

[31] Drelich JW. Contact angles: From past mistakes to new developments through liquid-solid adhesion measurements. Advances in Colloid and Interface Science. 2019;**267**:1-14

[32] Hosseini S, Savaloni H, Shahraki MG. Influence of surface morphology and nano-structure on hydrophobicity: A molecular dynamics approach. Applied Surface Science. 2019;**48515**:536-546

[33] Azimi A, Rohrs C, He P. Hydrodynamics-dominated wetting phenomena on hybrid superhydrophobic surfaces. Journal of Colloid and Interface Science. 2020; **5627**:444-452